An efficient optimization and comparative analysis of cascade refrigeration system using NH3 /CO2 and C3H8/CO2 refrigerant pairs

Patel, Vivek; Panchal, Deep; Prajapati, Anil; Mudgal, Anurag; Davies, Philip

DOI:
10.1016/j.ijrefrig.2019.03.001

Document Version
Peer reviewed version

Citation for published version (Harvard):
Patel, V, Panchal, D, Prajapati, A, Mudgal, A & Davies, P 2019, 'An efficient optimization and comparative analysis of cascade refrigeration system using NH_3 /CO_2 and C_3H_8/CO_2 refrigerant pairs', *International Journal of Refrigeration*, vol. 102, pp. 62-76. https://doi.org/10.1016/j.ijrefrig.2019.03.001

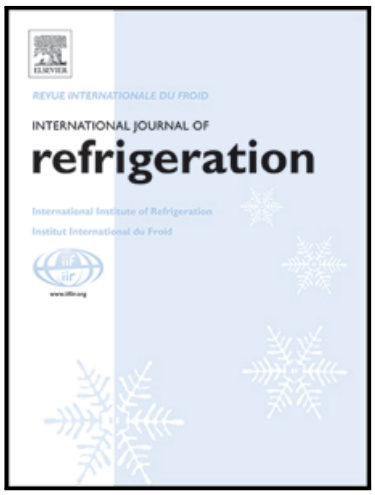

An efficient optimization and comparative analysis of cascade refrigeration system using NH_3 /CO_2 and C_3H_8/CO_2 refrigerant pairs

Vivek Patel , Deep Panchal , Anil Prajapati , Anurag Mudgal , Philip Davies

PII: S0140-7007(19)30097-0
DOI: https://doi.org/10.1016/j.ijrefrig.2019.03.001
Reference: JIJR 4308

To appear in: *International Journal of Refrigeration*

Received date: 20 September 2018
Revised date: 1 February 2019
Accepted date: 1 March 2019

Please cite this article as: Vivek Patel , Deep Panchal , Anil Prajapati , Anurag Mudgal , Philip Davies , An efficient optimization and comparative analysis of cascade refrigeration system using NH_3 /CO_2 and C_3H_8/CO_2 refrigerant pairs, *International Journal of Refrigeration* (2019), doi: https://doi.org/10.1016/j.ijrefrig.2019.03.001

Research Highlights

- Comparative analysis of NH_3/CO_2 and C_3H_8/CO_2 cascade refrigerating system is investigated
- Total annual cost and exergy destruction of system are considered for the comparative analysis
- Optimization problem of cascade refrigerating system is developed and solved
- Investigate the effect of operating parameters on the performance of cascade system
- Investigate the sensitivity of design variables on the performance of cascade system

An efficient optimization and comparative analysis of cascade refrigeration system using NH_3 /CO_2 and C_3H_8/CO_2 refrigerant pairs

Vivek Patel*

Department of Mechanical Engineering, Pandit Deendayal Petroleum University, Gujarat, India

E-mail: viveksaparia@gmail.com

Deep Panchal

Department of Mechanical Engineering, Pandit Deendayal Petroleum University, Gujarat, India

E-mail: deep.pmc14@sot.pdpu.ac.in

Anil Prajapati

Department of Mechanical Engineering, Pandit Deendayal Petroleum University, Gujarat, India

E-mail: anil.pmc14@sot.pdpu.ac.in

Anurag Mudgal

Department of Mechanical Engineering, Pandit Deendayal Petroleum University, Gujarat, India

E-mail: anurag.mudgal@pdpu.ac.in

Philip Davies

School of Engineering and Applied Science, Aston University, Birmingham B4 7ET, UK

E-mail: p.a.davies@aston.ac.uk

***Corresponding author**

Tel: +91 79 2327 5457;

Fax: +91 79 2327 5060

Abstract:

A cascade refrigeration system operating with CO_2 in the low temperature circuit and NH_3 as well as C_3H_8 in the high temperature circuit are investigated for the thermo-economic optimization. Optimization results are used for the comparative analysis of both the refrigerant pairs (NH_3/CO_2 vs. C_3H_8/CO_2). Optimization problem is formulated to minimize the total annual cost and exergy destruction of the system, and solved using a heat transfer search algorithm. Four operating parameters such as evaporator temperature, condenser temperature, condensing temperature of the low temperature circuit, and cascade temperature difference are investigated for the optimization. An application example of cascade refrigeration system is presented. Results are obtained in the form of Pareto-optimal points. Comparative results reveal that C_3H_8/CO_2 pair offered 5.33% lower cost and 6.42% higher exergy destruction compared to NH_3/CO_2 pair. The effect of design variables and its sensitivity to the performance of cascade system are also presented and discussed.

Keywords: Cascade refrigeration system; Exergy; Annualized cost; thermo-economic; optimization

Nomenclature

A_o Outer heat transfer area (m^2)

A_i Inner heat transfer area (m^2)

A_{min} Free flow area (m^2)

A_{fr} Frontal surface area (m^2)

C Cost ($)

C_{total} Total annual cost of plant ($)

c Unit cost of exergy ($/kW)

C_{el} Unit cost of input exergy ($/kW h)

CRF Capital Recovery Factor

CRS Cascade Refrigeration System

HTC High Temperature Circuit

LTC Low Temperature Circuit

VCR Vapor Compression Refrigeration

d_o Outer diameter of tube (m)

d_i Inner diameter of tube (m)

εx Specific exergy(J/kg)

$\dot{E}x$ Rate of exergy (kW)

$\dot{E}x_{Dest}$ Exergy Destruction (W)

f Friction coefficient

F Reynolds Number Factor

G Mass velocity (kg/m^{2}s)

h Specific enthalpy (kJ/kg)

H Operating hours per year (h)

k Thermal conductivity (W/m K)

L Length of tube (m)

$\dot{m}$ Mass flow rate (kg/s)

N Number of rows in fin-tube heat exchanger

P Pressure (Pa)

ΔP Pressure drop (kPa)

$\dot{Q}$ Heat transfer rate (W)

Q_{Air} Air flow rate (m^3/s)

R_p Pressure Ratio

S_g Specific gravity

T Temperature (°C)

U_o Overall heat transfer coefficient (W/m^2 K)

$\dot{W}_H$ Power compressor HTC (W)

$\dot{W}_L$ Power compressor LTC (W)

$\dot{W}_f$ Power fan (W)

x Vapour quality

X_{tt} Lockhart-Martinelli parameter

Greek symbols

η Exergetic efficiency

η_m Mechanical efficiency

η_{elec} Electrical efficiency

n_{isen} Free flow area/frontal area

μ Viscosity (Pa.s)

ρ Density (m^3/kg)

Subscripts

com Compressor

evp Evaporator

$cond$ Condenser

cas	Cascade
cr	Critical
$cold$	Cold space temperature
H	High temperature circuit
l	Liquid phase
g	Vapour phase
L	Low temperature circuit
me	Evaporating temperature HTC
mc	Condensing temperature LTC
Exp	Expansion valve
tot	Total

1. Introduction

In a Cascade Refrigeration System (CRS), two or more individual vapor compression refrigeration (VCR) circuits are coupled at the condenser-evaporator stages with heat transfer occurring between them. The CRS uses heat released from the condenser of one VCR circuit to vaporize the refrigerant in the other VCR circuit; thus heat transfer is wisely utilized and lower refrigeration temperature is attainable. If a single VCR circuit is used for low temperature application, the work input to compress the refrigerant will be high due to very high suction volume at compressor inlet. In contrast, CRS can be an effective option for -40^{o}C to -60^{o}C temperature applications [1]. Fig. 1(a) shows a CRS having two circuits: the high temperature circuit (HTC) and low temperature circuit (LTC). The evaporator of the LTC circuit maintains

the cold space temperature. CRS finds its application in rapid freezing systems and cold storages. It is also used in the upstream oil and gas sector for liquefaction of natural gas.

Nowadays there is a trend towards the use of natural refrigerants such as carbon dioxide, ammonia, propane, butane, ethane, due to the high global warming potential (GWP) and ozone depletion potential (ODP) of synthetic refrigerants based on halocarbons. Ammonia (NH_3) and propane (C_3H_8) have similar thermodynamic properties for use in refrigeration, and negligible ODP and GWP. The notable differences are the non-toxic nature and flammability of propane, whereas ammonia is toxic and corrosive to some metals [2]. Further, propane is safe and economical when used with right refrigeration system that complies with the safety codes and regulations for flammable refrigerants. However, propane has poor resistance to chlorinated solvents and aromatics. Also, it has a high thermal expansion coefficient which limits its high temperature applications. The NH_3/CO_2 pair has been delivering promising operational performance, with ammonia in the HTC and carbon dioxide in the LTC. Ammonia has sub-atmospheric pressure at temperatures below -35 ^{0}C, giving rise to a risk of air-leak into the evaporator, thus making it less suited to the LTC. In contrast, CO_2 has positive pressure at these temperatures making it an appropriate candidate for LTC [3]. It also has the benefits of being non-toxic and non-flammable.

There have been several recent studies using these refrigerant combinations. Bingming et al. [4] conducted the investigation on the performance of a NH_3/CO_2 CRS with twin-screw compressors. The authors analysed the effect of operating parameter on the COP of the system. Further, they carried out the comparison between experimental and theoretical value of the performance parameter of the system and observed 4 to 10% variation in COP. Dopazo et al. [1] performed the thermodynamic analysis of NH_3/CO_2 cascade refrigeration system. NH_3 is used in

high temperature stage and CO_2 in low temperature stage. The author developed an expression for obtaining the maximum COP of the system as a function cascade condenser temperature. Bhattacharyya et al. [2] demonstrated the performance trends of a C_3H_8/CO_2 cascade system with variation in design variables for simultaneous heating and cooling application. The authors reported that optimum value of intermediate temperature of the cascaded system decreases with increase in overlap temperature and with decrease in temperature approach. Lee et al. [3] carried out thermodynamic analysis of NH_3/CO_2 cascade refrigerator to obtained maximum COP and minimum exergy destruction of the system. The authors obtained the expression of system COP in terms of evaporator temperature, condenser temperature and cascade condenser temperature difference.

Agnew and Ameli [5] simulated a three-stage CRS to examine the performance of an alternative environmental friendly refrigerant pair. The authors considered R717 (ammonia) and R508b (46% R23 + 54% R116) pair and reported that the considered combination shows the improved performance over an original combination of R12 and R13. Aminyavari et al. [6] investigate NH_3/CO_2 cascade refrigeration system from exergetic, economic and environmental points of view by performing multi-objective optimization. The authors considered exergetic efficiency and the total cost rate of the system as an objective function and employed genetic algorithm as an optimization tool. Further, the authors reported an optimization results having 45.89% exergetic efficiency with total cost rate of 0.01099 US$. Rezayan and Behbahaninia [7] performed the thermo-economic optimization of NH_3/CO_2 cascade refrigeration system. The authors reported that for constant cooling capacity of 40 kW, a 9.34% reduction in total annual cost of the system observed compared to the base case design. Nasruddin et al. [8] performed thermo economic optimization of a cascade system having C_3H_8 in high temperature circuit and

mixture of C_2H_8+CO_2 in low temperature circuit. The authors obtained optimum operating temperature of the system that result in minimum exergy destruction (39876.04 W) and annual cost of the system ($51070.59.).

It can be concluded from the literature survey that very few researchers have carried out a systematic comparative analysis of refrigerant pairs as used in CRS. Moreover, the fundamental system design variables, such as temperatures in the various components of the CRS, have not yet been optimized in relation to the performance and cost of the system. In the present work, a comparative analysis of NH_3/CO_2 and C_3H_8/CO_2 refrigerant pairs has carried out from a thermo-economic viewpoint. Total exergy destruction and total annual cost of the system are considered as the objective functions. The multi-objective heat transfer search (MOHTS) algorithm is implanted to obtain Pareto solutions between conflicting objectives. Sensitivity of the system variables, namely evaporator temperature, condenser temperature, condensing temperature of LTC refrigerant and cascade condenser temperature difference has been investigated to identify their effects on the optimized value of cost and exergy destruction. Further, the effect of change in the operating variables on the objective function value of the system has also investigated. For simulation, the software tools REFPROP 9.1 for thermo-physical property values and MATLAB 2017b for optimization iterations have been integrated and implemented.

The remaining sections of the paper are organized as follows: Section 2 describes the thermo-economic modeling of cascade refrigeration system. Section 3 explains the objective function formulation and framework of system optimization. Section 4 describes the heat transfer search algorithm. Section 5 explains multi-objective heat transfer search algorithm. The application example, optimization results and comparative analysis are discussed in section 6. Finally, the conclusions are presented in section 7.

2. Thermo-economic modeling formulation

This section describes the thermal and economic modeling of cascade refrigeration system along with energy and exergy formulation.

2.1. Thermodynamic and exergy analysis

The thermal model developed uses the following assumptions:

(i) All the system components run under steady-state conditions.

(ii) The changes in kinetic and potential energy are negligible. Hence exergy is found from enthalpy and entropy.

(iii) Refrigerant leakage is negligible throughout.

The cooling load taken by evaporator to maintain required cold space temperature for plant is given by:

$$\dot{Q}_L = \dot{m}_L(h_1 - h_4) \tag{1}$$

Where $\dot{m}_L$ is the mass flow rate of refrigerant in LTC. Subscripts indicate positions in the system according to Fig. 1(b).

Work input to run the evaporator fan depends on the air flow rate ($\dot{Q}_{Air,evp}$) and pressure drop across the evaporator (ΔP_{evp}) and is given by:

$$\dot{W}_{fan,evp} = \dot{Q}_{Air,evp}\Delta P_{evp} \tag{2}$$

Exergy destruction in the evaporator is calculated as follows:

$$\dot{E}x_{Dest,evp} = \left(1 - \frac{T_o}{T_{cold}}\right)\dot{Q}_L + \dot{m}_L(\varepsilon x_4 - \varepsilon x_1) + \dot{W}_{fan,evp} \tag{3}$$

Where, $\dot{Q}_L$ is the heat transfer rate in low temperature circuit and εx is the specific exergy of the refrigerant.

Work input in form of electricity to run LTC compressor is given by:

$$\dot{W}_{LTC,com} = \frac{\dot{m}_L(h_{2s} - h_1)}{\eta_{isen}\eta_m\eta_{elec}} = \frac{\dot{m}_L(h_2 - h_1)}{\eta_m\eta_{elec}} \quad (4)$$

Where, η_{isen}, η_m, and η_{elec} are respectively the isentropic efficiency, mechanical efficiency and electrical efficiency of the compressor.

Exergy destruction in the LTC compressor is calculated as follows:

$$\dot{E}x_{Dest,LTC,com} = \dot{m}_L(\varepsilon x_1 - \varepsilon x_2) + \dot{W}_{LTC,com} \quad (5)$$

The exergy destruction in LTC and HTC expansion valves respectively are given by:

$$\dot{E}x_{Dest,LTC,Exp} = \dot{m}_L(\varepsilon x_3 - \varepsilon x_4) \quad (6)$$

$$\dot{E}x_{Dest,HTC,exp} = \dot{m}_H(\varepsilon x_7 - \varepsilon x_8) \quad (7)$$

Where,$\dot{m}_H$ is the mass flow rate of refrigerant in HTC.

The heat transfer in the cascade condenser is calculated as:

$$\dot{Q}_M = \dot{m}_H(h_5 - h_8) = \dot{m}_L(h_2 - h_3) \quad (8)$$

The exergy destruction associated with cascade condenser is given by:

$$\dot{E}x_{Dest,cas,cond} = \dot{m}_L(\varepsilon x_2 - \varepsilon x_3) + \dot{m}_H(\varepsilon x_8 - \varepsilon x_5) \quad (9)$$

The work input to condenser fan in form of electricity is given by:

$$\dot{W}_{fan,cond} = \dot{Q}_{Air,cond}\Delta P_{cond} \quad (10)$$

Where, $\dot{Q}_{Air,cond}$ is the air flow rate and ΔP_{cond} is the pressure drop across the condenser.

Exergy destruction in condenser is calculated as follows:

$$\dot{E}x_{Dest,cond} = \left(1 - \frac{T_o}{T_o}\right)\dot{Q}_H + \dot{m}_H(\varepsilon x_6 - \varepsilon x_7) + \dot{W}_{fan,cond} \quad (11)$$

Work input in form of electricity to run HTC compressor is given by:

$$\dot{W}_{HTC,comp} = \frac{\dot{m}_H(h_{6s} - h_s)}{\eta_{isen}\eta_m\eta_{elec}} = \frac{\dot{m}_H(h_6 - h_5)}{\eta_m\eta_{elec}} \quad (12)$$

Exergy destruction in LTC compressor is calculated as follows:

$$\dot{E}x_{Dest,HTC,com} = \dot{m}_H(\varepsilon x_5 - \varepsilon x_6) + \dot{W}_{HTC,com} \quad (13)$$

The isentropic efficiency of the HTC compressor is given by [7],

$$\eta_{isen} = 0.83955 - 0.01026\, R_{ph} - 0.00097 R_{ph}^2 \quad (14)$$

Where, R_{ph} is the pressure ratio of the HTC compressor

The isentropic efficiency of LTC compressor is given by [8],

$$\eta_{isen} = 0.89810 - 0.09238\, R_{pl} + 0.00476\, R_{pl}^2 \quad (15)$$

where, R_{pl} is the pressure ratio of the LTC compressor

The total exergy input to the system is given by,

$$\dot{E}x_{in} = \dot{W}_{HTC,com} + \dot{W}_{LTC,com} + \dot{W}_{fan,cond} + \dot{W}_{fan,evp} \quad (16)$$

Similarly, the total exergy output of system/ product exergy is the summation of exergy output of individual components:

$$\dot{E}x_{out} = \left(\frac{T_o}{T_{cold}} - 1\right)\dot{Q}_L \quad (17)$$

The total exergy destruction of the cascade system and the second law efficiency can be calculated by:

$$\dot{E}x_{Dest,tot} = \dot{E}x_{Dest,evp} + \dot{E}x_{Dest,LTC,com} + \dot{E}x_{Dest,LTC,Exp} + \dot{E}x_{Dest,HTC,exp} + \dot{E}x_{Dest,cas,cond} + \dot{E}x_{Dest,cond} + \dot{E}x_{Dest,HTC,com} \quad (18)$$

$$\eta = 1 - \frac{\dot{E}x_{Dest,tot}}{\dot{E}x_{in}} \quad (19)$$

2.2. Sizing of Heat Exchangers

There are three heat exchangers in the cascade refrigeration system: condenser in HTC, evaporator in LTC, and cascade condenser. Condenser and evaporator are air cooled cross flow fin-tube type whereas cascade condenser is a counter flow shell-tube type. The schematics of both the heat exchanger are shown in Fig. 1(c) and (d) respectively. The specifications of these

heat exchangers have been mentioned in Tables 1 and 2 respectively. The heat transfer area of a heat exchanger can be calculated using following expressions:

$$A_o = \frac{\dot{Q}}{U_o \Delta T} \tag{20}$$

Where, ΔT is the Log Mean Temperature Difference (LMTD) and U_o represents the overall heat transfer coefficient of heat exchanger and calculated using following formula:

$$\frac{1}{A_o U_o} = \frac{1}{A_o h_o} + \frac{\ln\left(\frac{d_o}{d_i}\right)}{2\pi k L} + \frac{1}{A_i h_i} \tag{21}$$

where, *h* is the convective heat transfer coefficient, *k* is the thermal conductivity and *d* is the pipe diameter.

The heat transfer coefficient during two-phase flow of refrigerant (h_c) is found as follows [9]:

$$h_c = 0.023 \frac{k_l}{d_i} {Re_l}^{0.8} {Pr_l}^{0.4} \left[(1-x)^{0.8} + \frac{3.8 x^{0.76} (1-x)^{0.04}}{\left(\frac{P_{sat}}{P_{cr}}\right)^{0.38}} \right] \tag{22}$$

where, Re is the Reynolds number, Pr is the Prandtl number, *x* is the vapour quality, P_{sat} and P_{cr} are the saturation and critical pressure respectively.

Furthermore, the boiling heat transfer coefficient (h_b) can be estimated using following equation [8]:

$$h_b = F(1-x)^{0.8} Nu_l \frac{k_l}{d_i} \tag{23}$$

Where, Nu_l is the Nusselt number and *F* is the factor for Reynolds number and calculated using the following equations [10]:

$$Nu_l = 0.023 {Re_l}^{0.8} {Pr_l}^{0.4} \tag{24}$$

$$F = \begin{cases} 2.35\left(\frac{1}{X_{tt}} + 0.213\right)^{0.736} & if\ \frac{1}{X_{tt}} > 0.1 \\ 1 & if\ \frac{1}{X_{tt}} \leq 0.1 \end{cases} \quad (25)$$

Where, X_{tt} is Lockhart-Martinelli parameter which finds application in two-phase flow heat transfer calculations and is given as follows:

$$X_{tt} = \left(\frac{1-x}{x}\right)^{0.9}\left(\frac{\rho_g}{\rho_l}\right)^{0.5}\left(\frac{\mu_l}{\mu_g}\right)^{0.1} \quad (26)$$

Where, $\rho$is the density and μ is the dynamic viscosity.

The condenser and evaporator are air-cooled. The air pressure drop (ΔP) across the compact fin-tube heat exchanger is given by [11, 12]:

$$\Delta P = \frac{fNV^2}{2} \quad (27)$$

Where, *N* is the number of tube rows in fin and tube heat exchanger, *V* is the flow velocity and *f* is the friction factor given by,

$$f = \begin{cases} Re^{-0.15}\left[0.176 + \frac{0.32b}{(a-1)^{0.43} + \frac{1.13}{b}}\right] & \text{for inline tubes} \\ Re^{-0.16}\left[1 + \frac{0.47}{(a-1)^{1.08}}\right] & \text{for staggered tubes} \end{cases} \quad (28)$$

Where, the value of parameter *a* and *b* are depend on the Reynolds number.

The fin efficiency of air-cooled evaporator and condenser is obtained using following equation [13]:

$$\eta_{fin} = C_2 \frac{K_1(mr_1)I_1(mr_{2c}) - I_1(mr_1)K_1(mr_{2c})}{I_0(mr_1)K_1(mr_{2c}) + K_0(mr_1)I_1(mr_{2c})} \quad (29)$$

Where, the right hand side of the equation contains the modified Bessel functions of the first kind and second kind.

2.3. Cost analysis

Capital cost of CRS involves the investment done in condenser, evaporator, HTC and LTC compressors and cascade condenser. The operational cost includes electricity consumption of LTC and HTC compressors, evaporator and condenser fans. The exclusion of expansion valves from the cost analysis doesn't affect significantly compared to other equipment. The total cost of the system over a definite time interval can be given as follows [7]:

$$C_{total} = \sum c_i \dot{E}x_{in} + \sum_m z_m = \sum c_o \dot{E}x_{out} \tag{30}$$

Where $c_i$represents the cost of input exergy, z_m is the capital cost of each equipment, $c_o$is the cost of product exergy.

The capital cost/equipment cost ($) of each component given by [14]

$$C_{HTC,com} = 9624.2W_H^{0.46} \tag{31}$$

$$C_{LTC,com} = 10167.5W_L^{0.46} \tag{32}$$

$$C_{cond} = 1397A_{o,cond}^{0.89} + 629.05W_{fan,cond}^{0.76} \tag{33}$$

$$C_{evp} = 1397A_{o,evp}^{0.89} + 629.05W_{fan,evp}^{0.76} \tag{34}$$

$$C_{cas,cond} = 2382.9A_{o,cas,cond}^{0.68} \tag{35}$$

Where, *W* is the work input in kW and *A* is the area in m^2.

Generally engineering economic analysis is carried out to assess the total annual cost of system in order to recover the investment over a period of years. For the same, capital recovery factor (CRF) is calculated as follows [15]:

$$CRF = \frac{i(1+i)^n}{(1+i)^n - 1} \tag{36}$$

Where *i* is the annual interest rate and *n* is number of years of operation. Finally using all above costs, the annual cost of system can be approximated as:

$$C_{total} = \left[C_{HTC,com} + C_{LTC,com} + C_{cond} + C_{evp} + C_{cas,cond}\right].CRF$$
$$+ C_{el}.H\left[\dot{W}_{HTC,com} + \dot{W}_{LTC,com} + \dot{W}_{fan,cond} + \dot{W}_{fan,evp}\right] \quad (37)$$

The next section presented the objective function formulation of the cascade system along with the framework of system optimization.

3. Objective function formulation and framework of system optimization

This section deals with the formulation of objective function and associated design variables and constrained. As said before, an efficient refrigeration system generally costs more and one needs to find a balance. Higher the exergy destruction of the system, more the energy is wasted in work that is not useful and therefore the efficiency of system is less which often cost more. In the present work, thermo-economic optimization is carried out by simultaneous consideration of total cost and exergy destruction of the system. Both the objective function need to minimize simultaneously. The results of a multi-objective optimization represented in the form of Pareto front and one can select any solution from the front based on their criteria. The multi-objective optimization problem can be written as follows:

$$min/max\ F(x) = [f_1(x),\ f_2(x)] \quad (38)$$

$$g(x) \leq 0;\quad h(x) = 0\ ;\ x_l < x < x_u \quad (39)$$

Where,$f_1(x)$and $f_2(x)$is the objective function that will be optimized (in the present work total cost and exergy destruction of the system), x is the decision variable/s that will be iterated to find the optimum value of the objective function, $g(x)$ and $h(x)$are the inequality and equality constraints of the optimization problem.

In the present work, four design variables which affect the performance of CRS are considered for optimization. These variables includes temperature of condenser (T_c), temperature

of evaporator (T_e), condensing temperature in cascade condenser (T_{mc}), and temperature difference between two refrigerants in cascade condenser (ΔT). The range for each variable considering the position of VCR cycle of refrigerants in p-h and T-s (temperature-entropy) diagrams is as follows:

$$30\,^{o}C \leq T_c \leq 70^{o}C \quad (40)$$

$$-56\,^{o}C \leq T_e \leq -46\,^{o}C \quad (41)$$

$$-13\,^{o}C \leq T_{mc} \leq 2\,^{o}C \quad (42)$$

$$2\,^{o}C \leq \Delta T \leq 12^{o}C \quad (43)$$

Design specification as well as associated constraints considered in the present work is listed in Table 3. Further, the overview of the whole optimization process can be seen in Fig. 2.

4. Heat transfer search (HTS) algorithm

The heat transfer search (HTS) algorithm is a population based algorithm developed by Patel and Savsani [16]. The algorithm works based on the law of thermodynamic and heat transfer. The HTS algorithm mimics the thermal equilibrium behaviour executed between system and surroundings. In the context of optimization, best solution represents the surrounding while remaining solutions composed the system. Combine system and surrounding formed the population of optimization algorithm. Any system always tries to achieve the state of surrounding by performing heat transfer between the system and surrounding. The mode of heat transfer many be conduction, convection or radiation. Likewise, each solution from the population is improved with the help of best solution or any other solution fromm the populations. The HTS algorithm composed of three phases, namely conduction phase, convection phase and radiation phase. Thus, the improvement in the solutions can take place by

executing any of this phase during the course of optimization. Further, each of this phase executed with the equal probability during the course of optimization. The working of each phase of the HTS algorithm describe below for maximization problem. Here, size of the population, number of design variables and generation number are denoted by '*n*', '*m*' and '*g*' respectively.

4.1. Conduction phase

This phase simulates the conduction heat transfer behaviour between system and surrounding or within the system. In this phase, the solution of the optimization problem improved with the help any randomly selected solution from the population. This randomly selected solution may or may not be a best solution. If the randomly selected solution is best solution then it is analogues to heat transfer between system and surrounding else it analogues to heat transfer with the system. The solutions are updated according to following equation during conduction phase.

$$\begin{cases} X_{j,i}^{new} = X_{k,i}^{old} - R^2 X_{k,i}^{old} & If\ f\left(X_j\right) < f\left(X_k\right) \\ X_{k,i}^{new} = X_{j,i}^{old} - R^2 X_{j,i}^{old} & If\ f\left(X_k\right) < f\left(X_j\right) \end{cases}; \quad If\ g \le g_{\max}/CDF \tag{44}$$

$$\begin{cases} X_{j,i}^{new} = X_{k,i}^{old} - r_i X_{k,i}^{old} & If\ f\left(X_j\right) < f\left(X_k\right) \\ X_{k,i}^{new} = X_{j,i}^{old} - r_i X_{j,i}^{old} & If\ f\left(X_k\right) < f\left(X_j\right) \end{cases}; \quad If\ g > g_{\max}/CDF \tag{45}$$

Where, $j=1,2,...,n$, $j \neq k$, $k \in (1,2,\ldots,n)$ and $i \in (1,2,\ldots,m)$. Further, k and i are randomly selected solution and design variables. R is the probability of the execution of conduction phase which is 0 - 0.3333 in the present case and g_{max} is the maximum number of generation. Furthermore, r_i is the uniformly distributed random number varies between 0 - 1 and CDF is the conduction factor. The value of CDF is taken as 2 in the present work.

4.2. Convection phase

This phase simulate the convection heat transfer behaviour between system and surrounding. Convection heat transfer takes place between mean temperature of the system and surrounding. Hence, in this phase, solution of the optimization problem improved with the help of mean solution and best solution of the population. Further, during the heat transfer, mean temperature of the system changes continuously. Likewise, during the course of optimization, mean solution of the population changes continuously. This change in mean solution is happened with the help of temperature change factor (TCF). The solutions are updated according to following equation during convection phase.

$$X_{j,i}^{new} = X_{j,i}^{old} + R * \left(X_s - X_{ms} * TCF \right) \tag{46}$$

$$\begin{cases} TCF = abs\left(R - r_i \right) & If\ g \le g_{\max} / COF \\ TCF = round\left(1 + r_i \right) & If\ g > g_{\max} / COF \end{cases} \tag{47}$$

Where, $j=1,2,\ldots,n$, $i=1,2,\ldots,m$. X_s is the design variable of best solution and X_{ms} is mean value of the design variable. R is the probability of the execution of convection phase which is 0.3333 – 0.6666 in the present case. Furthermore, r_i is the uniformly distributed random number varies between 0 - 1 and COF is the convection factor. The value of COF is taken as 10 in the present work.

4.3. Radiation phase

This phase simulate the radiation heat transfer behaviour between system and surrounding or within the system. In this phase, solution of the optimization problem improved with the help any randomly selected solution from the population. The solutions are updated according to following equation during radiation phase.

$$\begin{cases} X_{j,i}^{new} = X_{j,i}^{old} + R*\left(X_{k,i}^{old} - X_{j,i}^{old}\right) & If\ f\left(X_j\right) < f\left(X_k\right) \\ X_{j,i}^{new} = X_{j,i}^{old} + R*\left(X_{j,i}^{old} - X_{k,i}^{old}\right) & If\ f\left(X_k\right) < f\left(X_j\right) \end{cases}; \quad If\ g \le g_{\max}/RDF \tag{48}$$

$$\begin{cases} X_{j,i}^{new} = X_{j,i}^{old} + r_i*\left(X_{k,i}^{old} - X_{j,i}^{old}\right) & If\ f\left(X_j\right) < f\left(X_k\right) \\ X_{j,i}^{new} = X_{j,i}^{old} + r_i*\left(X_{j,i}^{old} - X_{k,i}^{old}\right) & If\ f\left(X_k\right) < f\left(X_j\right) \end{cases}; \quad If\ g > g_{\max}/RDF \tag{49}$$

Where, $j=1,2,...,n,\ j \neq k,\ k \in (1,2,...,n)$ and $i \in (1,2,\ldots,m)$. Further, k is a randomly selected solution. R is the probability of the execution of conduction phase which is 0.6666 - 1 in the present case. Furthermore, r_i is the uniformly distributed random number varies between 0 - 1 and RDF is the radiation factor. The value of RDF is taken as 2 in the present work.

5. Multi-objective heat transfer search (MOHTS) algorithm

Multi-objective heat transfer search (MOHTS) algorithm is a multi-objective version of the heat transfer search algorithm [17-19] which can handle two or more than two conflicting objective functions simultaneously. The non-dominated solutions generated by the MOHTS algorithm are stored in the external archive. Further, domination of solutions kept in the archive is check with the help of ε-dominance based updating method [20]. These non-dominated solutions kept in the external archive are used obtained Pareto front in MOHTS algorithm.

The archiving process in MOHTS algorithm employed grid based approach with fixed size archive. The archive stored the best solutions obtained during the execution of HTS algorithm. Further, the archive is update in every generation during the execution of the HTS algorithm by adapting ε-dominance method. The ε-dominance method adopted in the MOHTS algorithm presumes a space having dimensions equal to the number of objectives of the optimization problem. This space further converted into the boxes of ε to ε size by slicing each dimension. Each box hold the solutions generated during the course of optimization. After that,

the boxes which are dominated by the other boxes are removed first. Thus, the solutions in those boxes are removed. Afterward, in the remaining box if more than one solution exists then the dominated ones are removed from that box. Therefore, only one solution remains in the box which is non-dominated in nature. Thus, only non-dominated solutions are retained in the archive.

The next section describes the application example and results-discussion of the considered cascade system.

6. Application example and results-discussion

An application example of CRS is analyzed for thermo-economic optimization. NH_3/CO_2 and C_3H_8/CO_2 refrigerant pair is considered for the investigation for comparative analysis. Temperature-dependent thermophysical properties values of both the fluids are considered during the optimization procedure. So, the objectives are to find out the design parameter of the CRS (i.e. evaporator temperature, condenser temperature, condensing temperature of LTC refrigerant, and cascade temperature difference) for minimum total cost and exergy destruction of the system. The effect of refrigeration load on the thermo-economic function is examined. Further, the effect of design variables on cost and exergy destruction as well as sensitivity of design variables is also investigated.

Initially, single objective optimization of both objective functions is carried out to identify its behaviour with respect to each other. The control parameters of HTS and MOHTS algorithm used in the present investigation are listed in Table 4. The refrigeration load of the CRS is 40 kW, evaporator temperature is -45 ^{0}C, and ambient temperature is 25 ^{0}C. Results of the single objective optimization for NH_3/CO_2 and C_3H_8/CO_2 refrigerant pair are demonstrated in

Table 5. It can be observed from the results that minimum cost is obtained when exergy destruction is highest and vice versa. Overall, the results of single objective optimization reveal the conflict between total cost and exergy destruction. So, multi-objective optimization is carried out between conflicting objective function with the help of MOHTS algorithm

For the considered example of the CRS, 100 design points are generated as Pareto optimal points during multi-objective optimization. Fig. 3 shows the distribution of Pareto optimal points in two-dimensional objective space when the refrigeration load is 40 kW. It can be observed from the figure that for minimum exergy destruction design (upper left corner of Fig. 3), C_3H_8/CO_2 pair turns out to be more costly than NH_3/CO_2 pair at fixed exergy destruction value. For minimum total cost design (bottom right corner of Fig. 3), NH_3/CO_2 turns out to be more costly compared to C_3H_8/CO_2 pair at any given value of exergy destruction. Design variables value of some selected Pareto points of Fig. 3 are displayed in Table 6 along with objective function value. For NH_3/CO_2 refrigerant pair, 36.64% reduction in total cost with 59.38% increase in exergy destruction is observed between point A and F of Pareto solutions. This behaviour is observed due to rise in cascade temperature difference, condenser temperature and evaporator temperature while moving from design point A to F. Similarly, for C_3H_8/CO_2 refrigerant pair, the change in total cost and exergy destruction is 42.58% and 61.27% respectively between point A and F of Pareto solutions. Further, decision making method namely TOPSIS is utilizes in order to select best solution from Pareto optimal points. Detail description related to working of TOPSIS method is available in the literature [21, 22]. The final solutions selected by the TOPSIS method is shown in Fig. 3 and listed in Table 7.

Fig. 4 demonstrates the effect of refrigeration load on the Pareto optimal solution of NH_3/CO_2 and C_3H_8/CO_2 refrigerant pair. It can be clearly observed that there is a noticeable shift

of Pareto-front for both the refrigerants when load changes. Immediate change that can be pointed out is that optimum values of exergy destruction and cost increase with increasing load. It is interesting to note that the relative behavior of Pareto-fronts of refrigerant pairs remains same even if the load changes. Few Pareto optimal solution points of refrigerant pairs overlap each other at almost halfway length of the Pareto front curve. Further, it can be observed that the spread of multi-objective optimal points is also more when load increases.

Fig. 5(a) - 5(d) shows the effect of design variables on the exergy destruction for both the refrigerants pair. It can be observed from Fig. 4(a) that increasing the evaporator temperature reduces the exergy destruction of the refrigeration system. The effect of condenser temperature and cascade temperature difference on exergy destruction of the system is shown in Fig. 5(b) and 5(c) respectively. It can be observed from the figure that the exergy destruction of the refrigeration system increases with the rise in condenser temperature and cascade temperature difference. Further, for any given evaporator temperature, condenser temperature, or cascade temperature difference the exergy destruction of C_3H_8/CO_2 pair is more as compared to NH_3/CO_2 pair. Fig. 5(d) shows the effect of condensing temperature of LTC on exergy destruction of the system. It can be observed from the figure that the exergy destruction of C_3H_8/CO_2 pair is increases with the rise in condensing temperature of LTC. However, the exergy destruction of NH_3/CO_2 pair is reduces initially and reached at certain minimum value with the increment in condensing temperature of LTC. Afterwards, further increment in the condensing temperature of LTC increases the exergy destruction of NH_3/CO_2 pair.

Fig. 6(a) – 6(h) shows the effect of design variables on the cost of each component of the system for both the refrigerant pair. It can be observed from Fig. 6(a) and 6(b) that noticeable change occurs in the cost of the evaporator as compared to other components with variation in

evaporator temperature for both the refrigerant pair. Lower the evaporator temperature, higher the temperature difference between the refrigerant and cold space requiring lesser heat transfer area. This decreases the evaporator cost. On the other end, the cost of compressor and condenser is increased due to rise in pressure ratio and mass flow rate of refrigerant with the reduction in evaporator temperature. Fig. 6(c) and 6(d) shows the effect of condenser temperature. It can be observed that condenser cost is decreases with rise in condenser temperature. Since, the logarithmic temperature difference (LMTD) of the condenser is increases with the rise in condenser temperature which reduces the area required for condenser and hence cost associated with the condenser. However, the higher condenser temperature increases the pressure ratio (P_6/P_5) which in turn increases the HTC compressor work.

Fig. 6(e) and 6(f) show the effect of condensing temperature of LTC refrigerant (T_{mc}) on cost of each component for both the refrigerant pair. It can be observed from the figure that the costs of various components do not vary noticeably with variation in T_{mc} as they do with T_e and T_c. The LTC compressor work increases with rise in T_{mc} due to rise in pressure ratio P_2/P_1. However, HTC compressor work will reduces with the rise in T_{mc} due to reduction in pressure ratio P_6/P_5. Increase in T_{mc} shows an increasing trend in the condenser cost while decreasing trend in evaporator cost. T_{mc} doesn't affect cascade condenser cost since temperature difference is constant. Fig. 6(g) and 6(h) shows the effect of cascade temperature difference (ΔT). It can be observed from the figure that the cascade condenser cost decreases with rise in ΔT due to rise in LMTD value. Further, higher ΔT values push T_{mc} and T_{me} apart (high T_{mc}, low T_{me}) causing high compressor costs. Since the duty of HTC compressor increases due to higher pressure ratio P_6/P_5, the condenser cost can also be observed to be increasing with ΔT.

Fig. 7(a) – 7(d) shows the effect of the design variables on the total cost of cascade refrigeration system for both the refrigerant pair. The dominant effect of evaporator cost on the total cost of the system with variation in evaporator temperature (T_e) can be easily observed in Fig. 7(a) for both the refrigerant pair. The effect of condenser temperature (T_c) on total cost of the system is shown in Fig. 7(b). With the increase in condenser temperature, total cost of the system reduces and reaches at minimum value. Further increment in condenser temperature, increases the total cost of the system. Similar behaviour is observed on total cost of the system (Fig. 7(c) and 7(d)) with increase in condensing temperature of LTC refrigerant (T_{mc}) and cascade temperature difference (ΔT). Fig. 6 also shows the optimum value of T_c, T_{mc} and ΔT where the total cost of the system is minimum.

An investigation is also carried out to identify the effect of decision variables on the optimum design. Pareto points A-F of Fig.3 (for both refrigerant pair) are considered in this investigation. Fig. 8(a) – 8(h) indicates the effect of design variables on the selected Pareto points for NH_3/CO_2 and C_3H_8/CO_2 refrigerant pair.

Fig. 8(a) and 8(b) presents the effect of evaporator temperature (T_e) on the optimized design of NH_3/CO_2 and C_3H_8/CO_2 refrigerant pair respectively. It can be seen from the figure that with the increase in evaporator temperature, reduction in the exergy destruction with the simultaneous rise in total cost of the system is observed. Also, the influence of T_e is pronounced more on total cost than exergy destruction. Fig 8(c) and 8(d) indicate the effect of condenser temperature (T_c) on the optimized design of both the refrigerant pair. It can be seen from the figure that with the increase in condenser temperature, reduction in the total cost with simultaneous rise in the exergy destruction of the system is observed. However, T_c has an almost equal influence on cost and exergy destruction. The effect of condensing temperature of LTC

refrigerant (T_{mc}) on the optimized design of refrigerant pair is shown in Fig. 8(e) and 8(f). It can be observed from the figure that total cost and exergy destruction of the system increases almost linearly with the rise in T_{mc}. The effect of cascade temperature difference (ΔT) on the Pareto points of both the refrigerant pair is shown on Fig. 8(g) and 8(h). It can be observed from the figure that ΔT has more influence on exergy destruction than total cost of the system.

Distribution of design variables corresponding to Pareto optimal points of Fig. 3 is shown in Fig. 9 for NH_3/CO_2 and C_3H_8/CO_2 refrigerant pair. It can be observed from the figure that optimum value of condensing temperature of LTC refrigerant almost remain invariable. Thus, the effect of this design variable is not significant in obtaining Pareto optimal solutions between total cost and exergy destruction of the system. However, scatter distribution of the evaporator temperature, condenser temperature and cascade condenser temperature difference is observed for Pareto solutions. Thus, these design variables produced conflicting behaviour between thermo-economic objectives of the cascade refrigeration system.

7. Conclusion

Thermo-economic optimization and comparative analysis of a two-stage cascade refrigeration having NH_3/CO_2 and C_3H_8/CO_2 refrigerant pairs are presented. The thermo-economic optimization problem is formed by considering total cost and exergy destruction of the system simultaneously. Four operating variables are investigated for the optimization. MOHTS has been employed to obtained Pareto-optimal solutions between conflicting objectives. In general, 36.64% reduction in total cost with 59.38% increase in exergy destruction is observed between extreme design points of Pareto front for NH_3/CO_2 refrigerant pair. Likewise, for C_3H_8/CO_2 refrigerant pair, the change in total cost and exergy destruction is 42.58% and 61.27%

respectively. Overall, the C_3H_8/CO_2 pair offered 5.33% less cost at 6.42% more exergy destruction compared to NH_3/CO_2 pair. A final optimal solution is selected from the Pareto optimal points using TOPSIS decision-making method. Distribution of each design variables corresponding to Pareto optimal solution points is also presented. Results revealed the level of conflict between thermo-economic objectives. Evaporator temperature, condenser temperature, and cascade temperature difference are found to be important operating parameters which caused a strong conflict between the objective functions. Further, sensitivity of design variables to the optimized value of thermo-economic function is also presented. Temperature difference in the cascade condenser is observed more sensitive to optimized value of objective function as compared to other variables.

References

[1] J.A. Dopazo, J.F. Seara, J. Sieres, F.J. Uhía, Theoretical analysis of a CO_2/NH_3 cascade refrigeration system for cooling applications at low temperatures, Appl. Thermal Eng. 29 (8–9) (2009) 1577-1583

[2] S. Bhattacharyya, S. Mukhopadhyay, A. Kumar, R.K. Khurana, J. Sarkar, Optimization of a CO2–C3H8 cascade system for refrigeration and heating, Int. J. of Refrig. 28 (2005) 1284-1292

[3] T.S. Lee, C.H. Liu, T.W. Chen, Thermodynamic analysis of optimal condensing temperature of cascade-condenser in CO_2/NH_3 cascade refrigeration systems, Int. J. Refrig. 29 (2006) 1100–1108.

[4] W. Bingming, W. Huagen, L. Jianfeng, X. Ziwen, Experimental investigation on the performance of NH_3/CO_2 cascade refrigeration system with twin-screw compressor, Int. J. Refrig. 32 (2009) 1358–1365

[5] B. Agnew, S.M. Ameli, A finite time analysis of a cascade refrigeration system using alternative refrigerants, Appl. Therm. Eng. 24 (17-18) (2004) 2557–2565.

[6] M. Aminyavari, B. Najafi, A. Shirazi, F. Rinaldi, Exergetic, economic and environmental (3E) analyses, and multi-objective optimization of a CO_2/NH_3 cascade refrigeration system, Appl. Thermal Eng. 65 (1–2) (2014) 42–50.

[7] R. Rezayan, A. Behbahaninia, Thermoeconomic optimization and exergy analysis of CO_2/NH_3 cascade refrigeration systems, Energy 36 (2011) 888–895.

[8] Nasruddin, S. Sholahudin, N. Giannetti, Arnas, Optimization of a cascade refrigeration system using refrigerant C3H8 in high temperature circuits (HTC) and a mixture of C2H6/CO2 in low temperature circuits (LTC), Appl. Thermal Eng. 104 (2016) 96–103.

[9] R.K. Shah, D.P. Sekulic, Fundamentals of Heat Exchanger Design, John Wiley & Sons, New Jersey, 2003.

[10] W. Chen and X. Fang, A note on the Chen correlation of saturated flow boiling heat transfer, Int. J. Refrig. 48 (2014) 100-104.

[11] E.C. Huge, Experimental investigation of effects of equipment size on convection heat transfer and flow resistance in cross flow of gases over tube banks, Trans. ASME 59 (1937) 573–581.

[12] O.L. Pierson, Experimental investigation of the influence of tube arrangement on convection heat transfer and flow resistance in cross flow of gases over tube banks, Trans. ASME 59 (1937) 563–572.

[13] Y.A. Cengel, A.J. Ghajar, Heat and Mass Transfer: Fundamentals and Applications, 5th ed., McGraw Hill Education, New Delhi, 2016.

[14] R. Smith, in: Chemical Process: Design and Integration, second ed., John Wiley & Sons, New York, 2005.

[15] A. Bejan, G. Tsatsaronis, M. Moran, Thermal Design and Optimization, John Wiley & Sons, New York, 1996.

[16] V.K. Patel, V.J. Savsani, Heat transfer search (HTS): A novel optimization algorithm, Inform Science 324 (2015) 217-246.

[17] V.K. Patel, V.J. Savsani, A. Mudgal, Many-objective thermodynamic optimization of Stirling heat engine, Energy 125 (2017) 629-642.

[18] V.K. Patel, V.J. Savsani, A. Mudgal, Efficiency, thrust, and fuel consumption optimization of a subsonic/sonic turbojet engine, Energy 144 (2018) 992-1002.

[19] B.D. Raja, R.L. Jhala, V.K. Patel, Multi-objective thermal-hydraulic optimization of a plate heat exchanger, Int. J. Therm. Sci. 124 (2018) 522-535

[20] K. Deb, M. Mohan, S. Mishra, Evaluating the epsilon-domination based multi-objective evolutionary algorithm for a quick computation of Pareto-optimal solutions, Evolutionary Computation 13 (2005) 501–525.

[21] D.L. Olson , Decision aids for selection problems, Springer, New York, 1996.

[22] C.L. Hwang, K. Yoon, Multiple attribute decision making: methods and applications a state-of-the-art survey, vol. 186, Springer Science & Business Media, 2012

Figure Caption

Fig. 1: (a) Schematic diagram of a two stage cascade refrigeration system. (b) *p-h* diagram of a typical two-stage cascade refrigeration system. (c) Schematic of typical tube-fin heat exchanger (d) Schematic of typical shell-tube heat exchanger.

Fig. 2: Optimization framework of CRS

Fig. 3: Variation of total cost and exergy destruction during thermo-economic optimization of CRS for both refrigerants pair

Fig.4: Effect of refrigeration load on Pareto optimal solutions of CRS for both refrigerants pair

Fig. 5: Effect of design variables on the exergy destruction of CRS for both the refrigerant pairs ((a) evaporator temperature, (b) condenser temperature, (c) condensing temperature of low temperature circuit, and (d) cascade temperature difference)

Fig. 6: Effect of design variables on the cost of an individual component of CRS for both the refrigerant pairs. ((a) & (b) evaporator temperature, (c) & (d) condenser temperature, (e) & (f) condensing temperature of low temperature circuit, and (g) & (h) cascade temperature difference)

Fig. 7: Effect of design variables on the total cost of CRS for both the refrigerant pairs ((a) evaporator temperature, (b) condenser temperature, (c) condensing temperature of low temperature circuit, and (d) cascade temperature difference)

Fig.8: Sensitivity of design variables to the optimized value of the multi-objective function for both the refrigerant pairs

Fig. 9: Distribution of design variable during multi-objective optimization of CRS for both the refrigerant pairs. ((a) & (b) evaporator temperature, (c) & (d) condenser temperature, (e) & (f)

condensing temperature of low temperature circuit, and (g) & (h) cascade temperature difference)

Table Caption

Table 1: Specifications of condenser and evaporator

Table 2: Specifications of cascade condenser

Table 3: Operating and economic parameters of the system

Table 4: Control Parameters of HTS and MOHTS algorithm

Table 5: Single objective optimization results

Table 6: Optimal parameters for sample design point (A-F) during thermo-economic optimization of CRS for both the refrigerant pairs

Table 7: Optimum results selected by TOPSIS method for both the refrigerant pairs

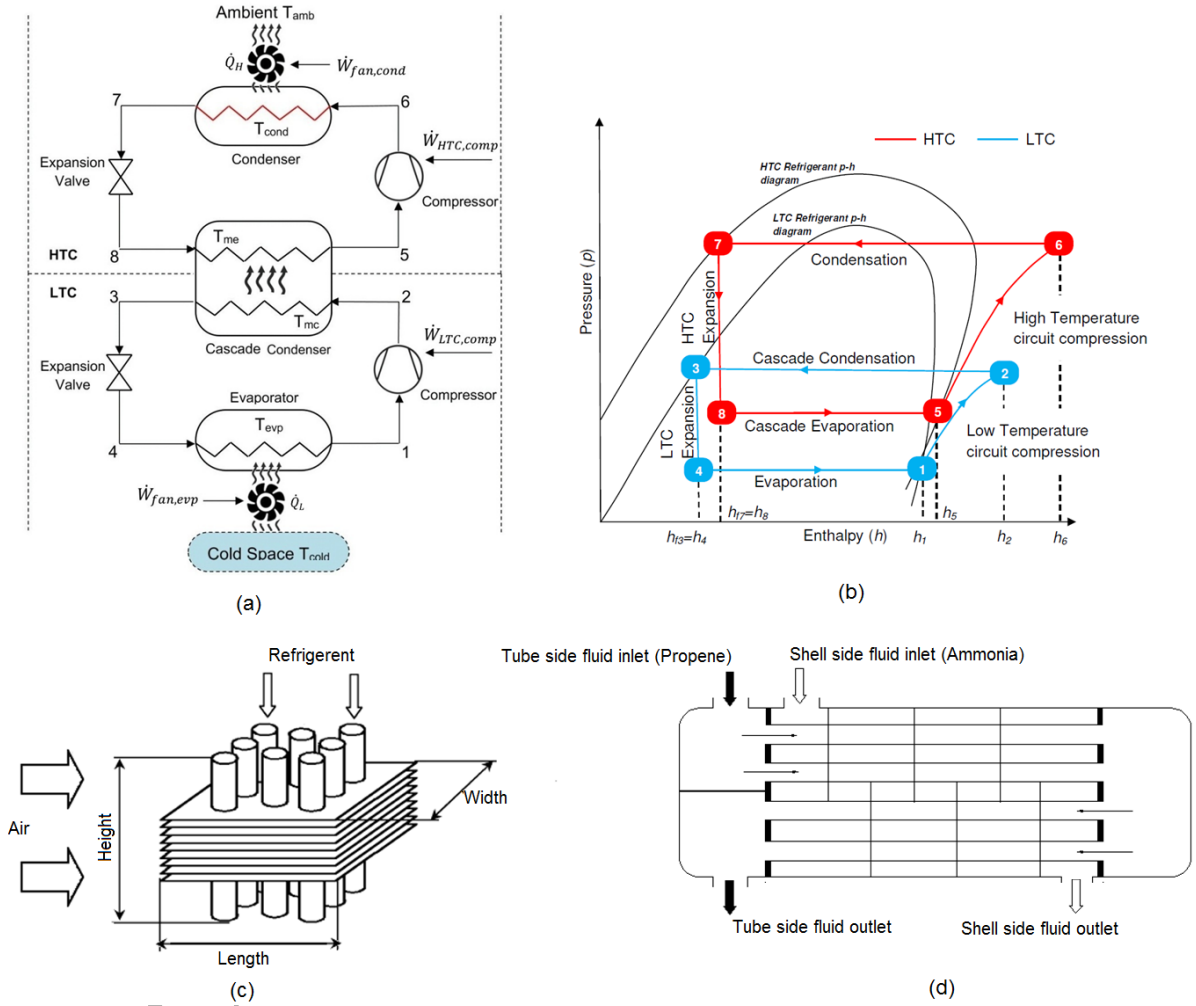
Ambient T_{amb}
$\dot{Q}_H$
$\dot{W}_{fan,cond}$
7
6
T_{cond}
Condenser
$\dot{W}_{HTC,comp}$
Expansion Valve
Compressor
HTC
8
T_{me}
5
LTC
3
2
T_{mc}
Cascade Condenser
$\dot{W}_{LTC,comp}$
Expansion Valve
Compressor
Evaporator
T_{evp}
4
1
$\dot{W}_{fan,evp}$
$\dot{Q}_L$
Cold Space T_{cold}
(a)
HTC
LTC
HTC Refrigerant p-h diagram
LTC Refrigerant p-h diagram
Pressure (p)
Condensation
HTC Expansion
High Temperature circuit compression
Cascade Condensation
LTC Expansion
Cascade Evaporation
Low Temperature circuit compression
Evaporation
$h_7=h_8$
h_5
$h_3=h_4$
Enthalpy (h)
h_1
h_2
h_6
(b)
Refrigerent
Air
Height
Width
Length
(c)
Tube side fluid inlet (Propene)
Shell side fluid inlet (Ammonia)
Tube side fluid outlet
Shell side fluid outlet
(d)

Fig. 1

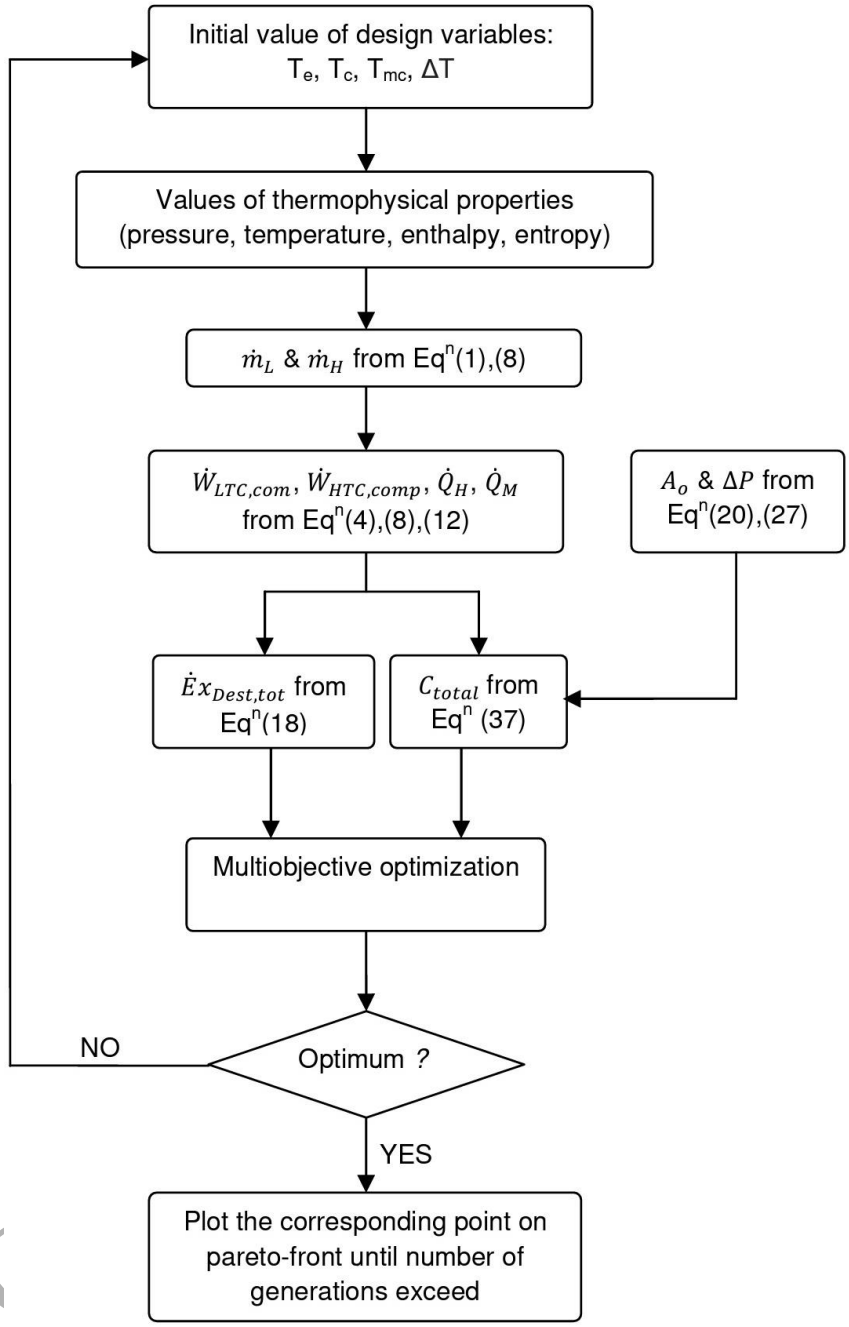
Initial value of design variables:
T_e, T_c, T_{mc}, ΔT
Values of thermophysical properties
(pressure, temperature, enthalpy, entropy)
$\dot{m}_L$ & $\dot{m}_H$ from Eq^n(1),(8)
$\dot{W}_{LTC,com}$, $\dot{W}_{HTC,comp}$, $\dot{Q}_H$, $\dot{Q}_M$
from Eq^n(4),(8),(12)
A_o & ΔP from
Eq^n(20),(27)
$\dot{E}x_{Dest,tot}$ from
Eq^n(18)
C_{total} from
Eq^n (37)
Multiobjective optimization
NO
Optimum ?
YES
Plot the corresponding point on
pareto-front until number of
generations exceed

Fig.2

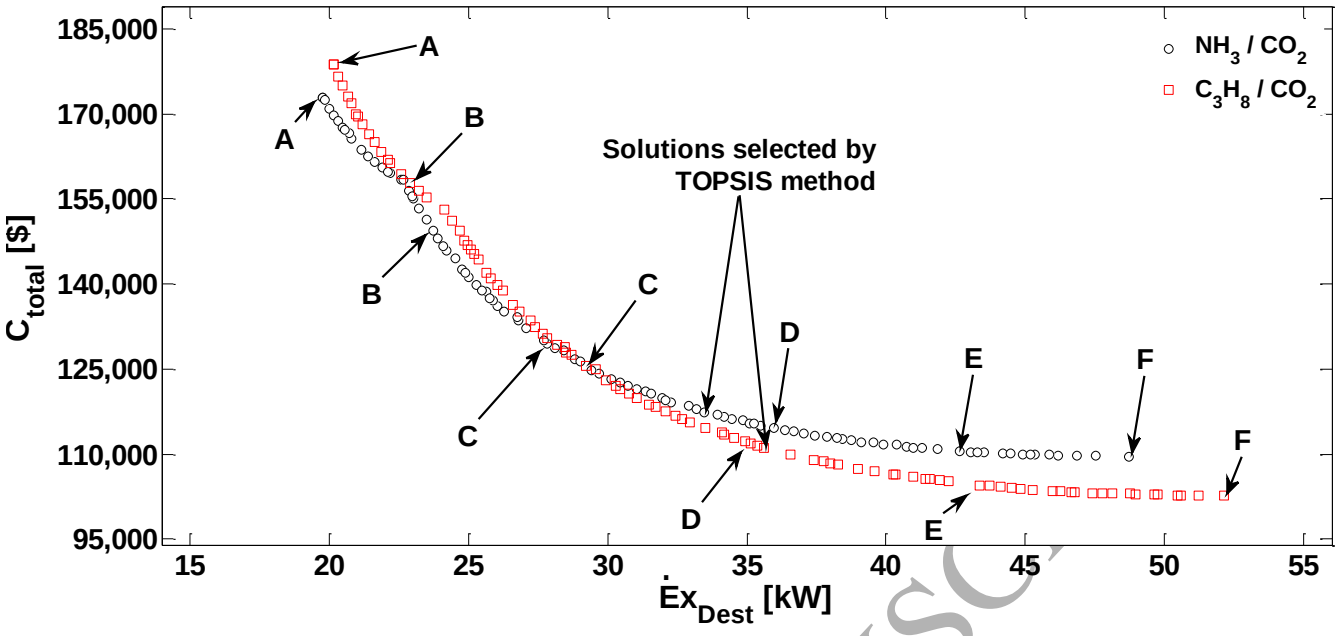

Fig 3

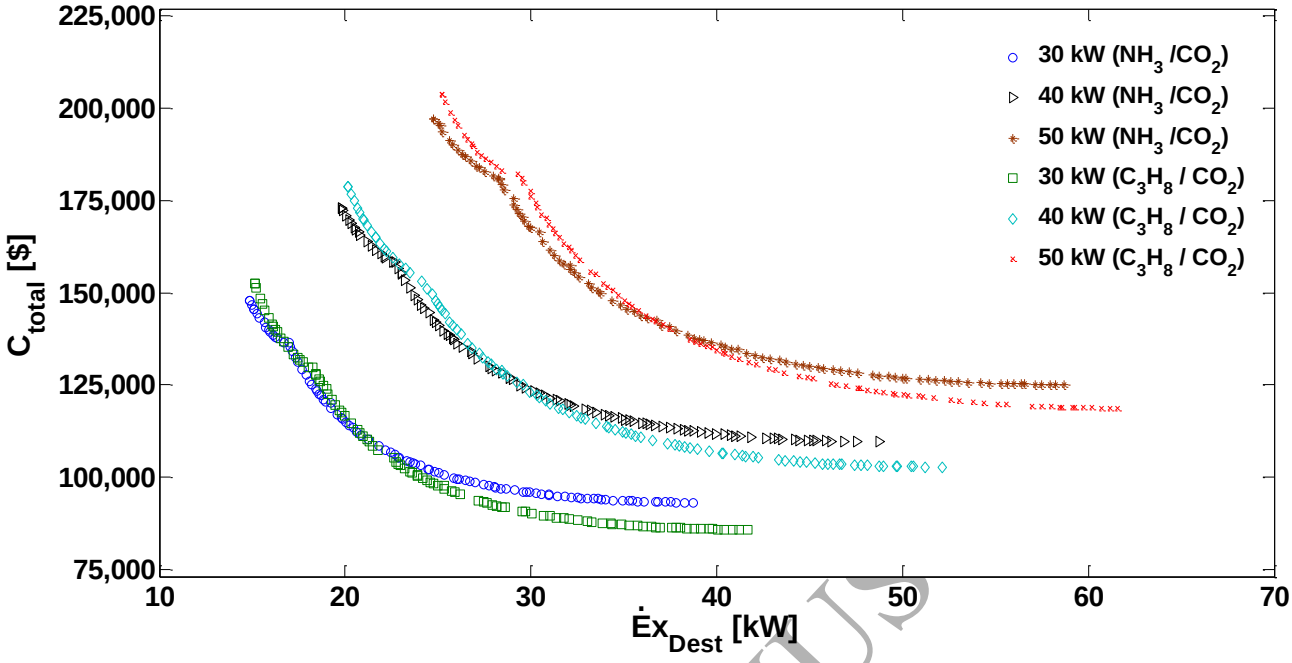

Fig. 4

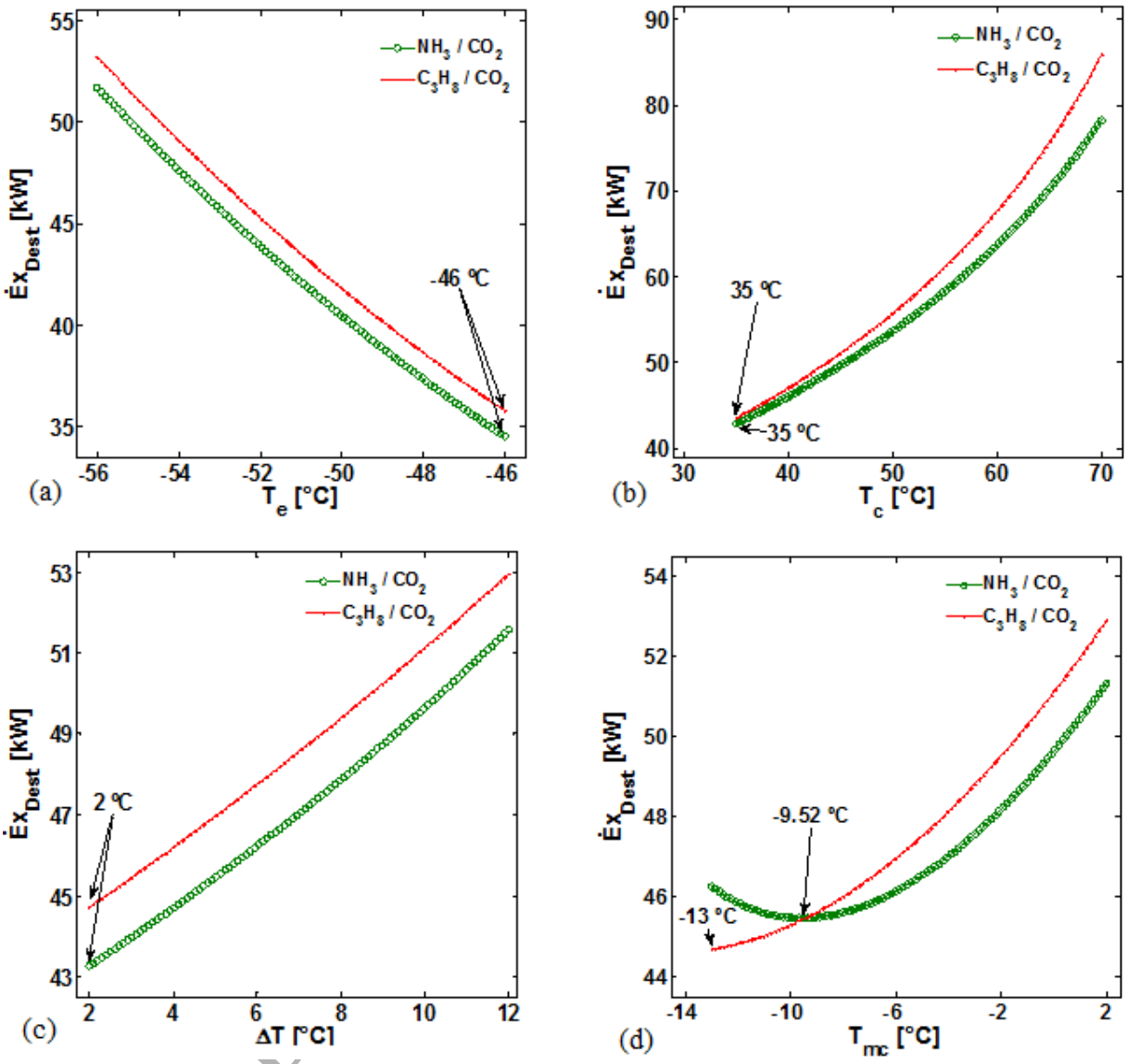

Fig. 5

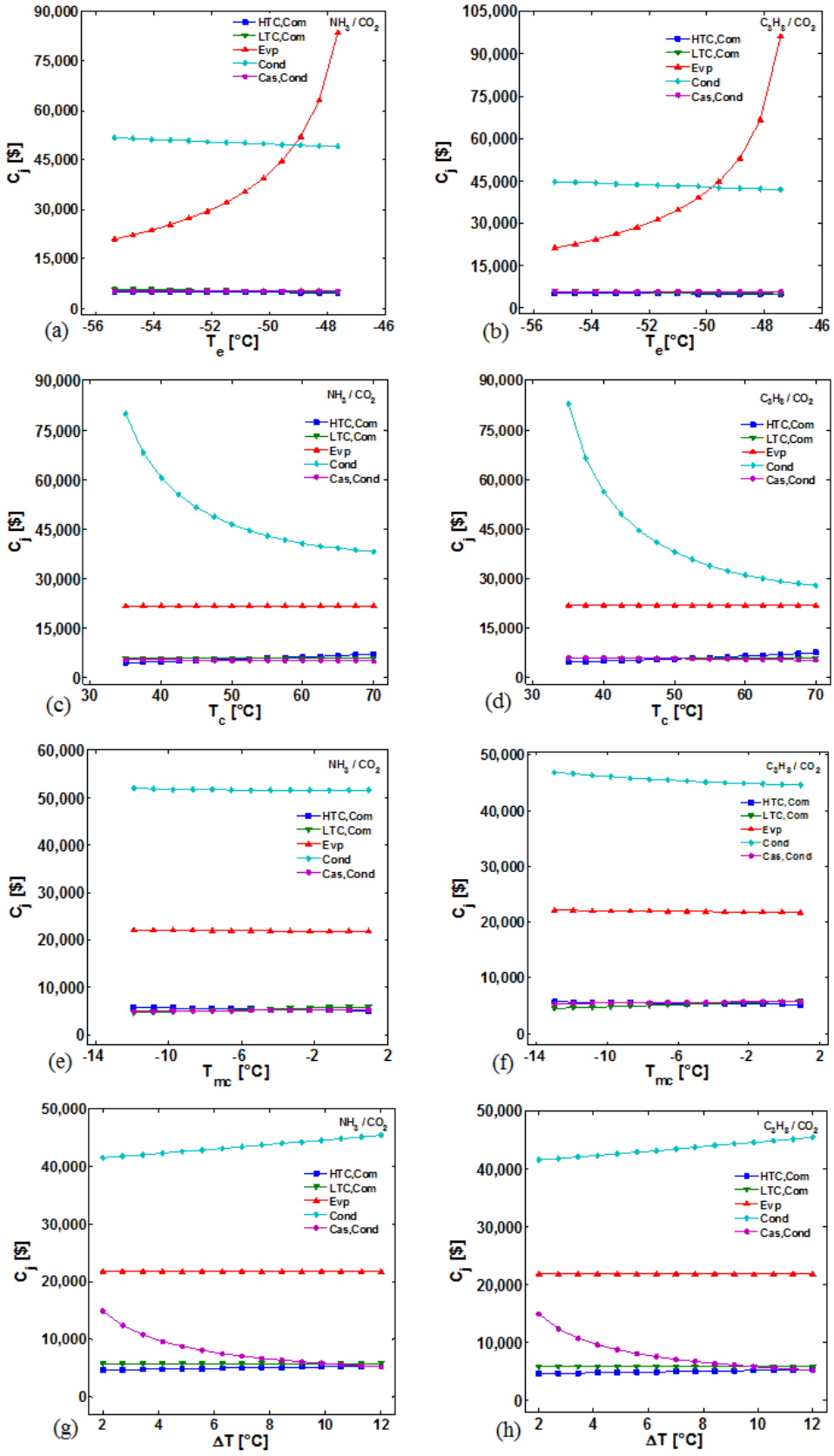
(a)
(b)
(c)
(d)
(e)
(f)
(g)
(h)
HTC,Com
LTC,Com
Evp
Cond
Cas,Cond
NH3 / CO2
C3H8 / CO2
Cj [$]
Te [°C]
Tc [°C]
Tmc [°C]
ΔT [°C]

Fig. 6

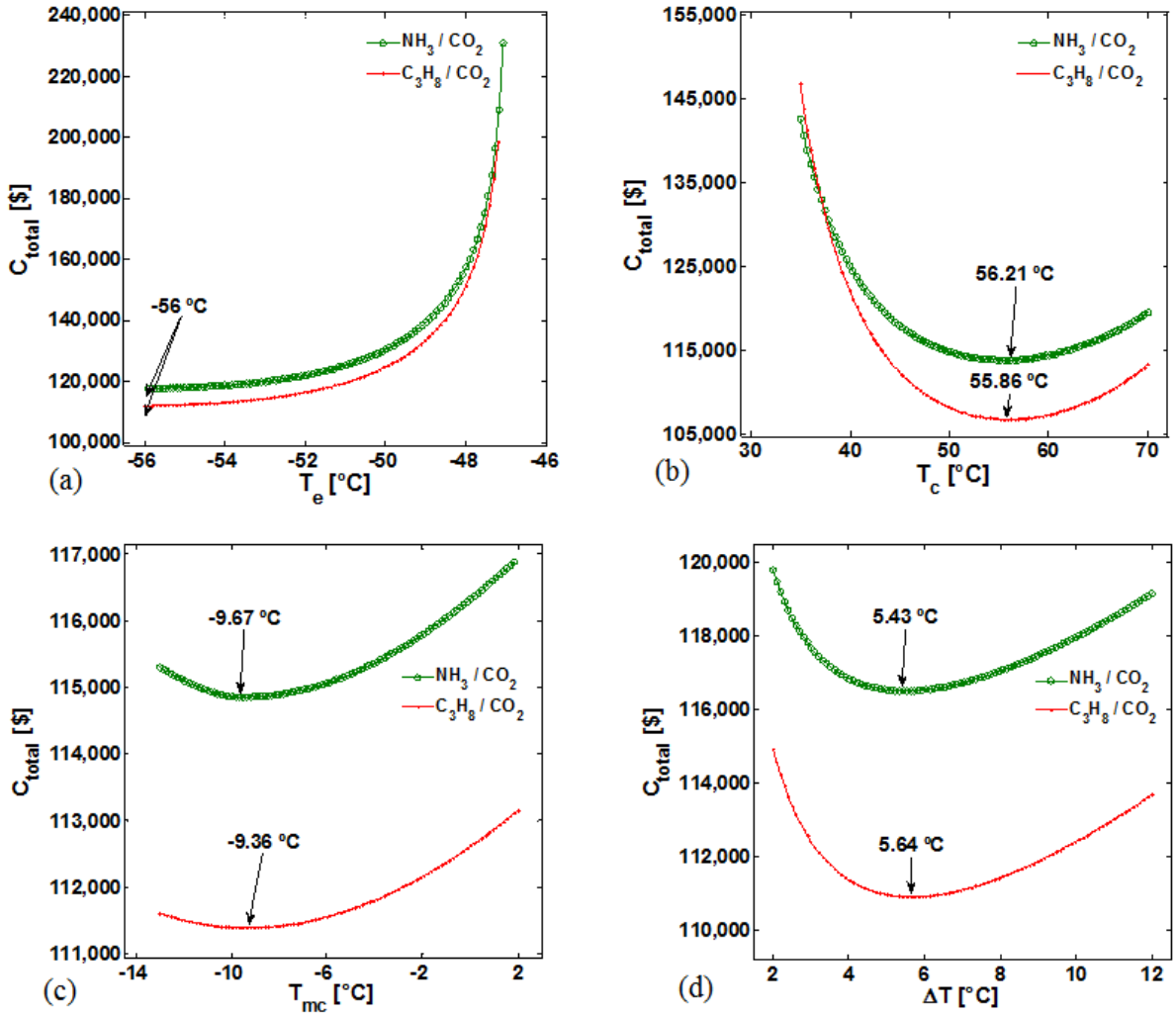

Fig. 7

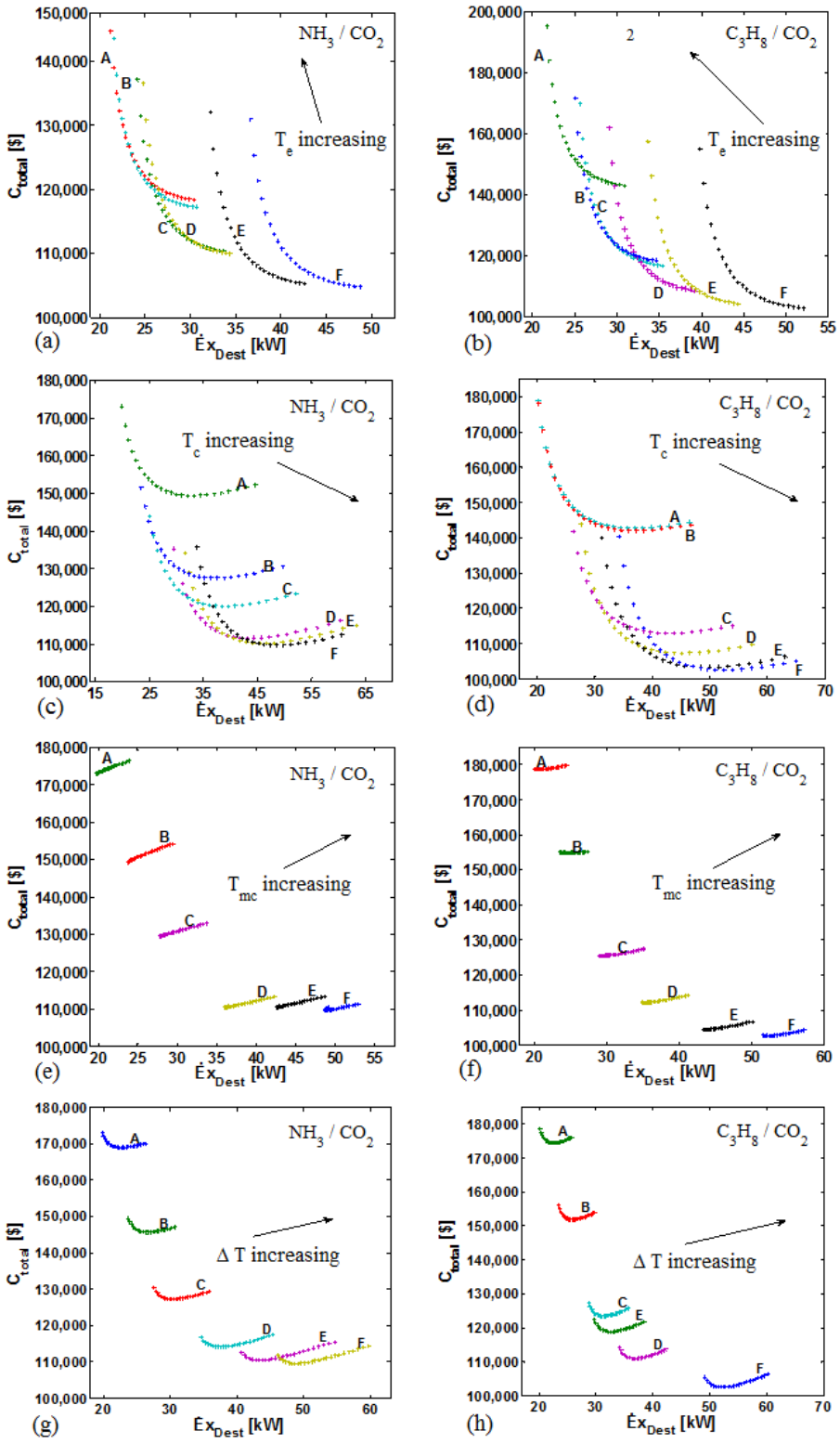
NH3 / CO2
T_e increasing
C3H8 / CO2
T_e increasing
NH3 / CO2
T_c increasing
C3H8 / CO2
T_c increasing
NH3 / CO2
T_mc increasing
C3H8 / CO2
T_mc increasing
NH3 / CO2
Δ T increasing
C3H8 / CO2
Δ T increasing
C_total [$]
Ėx_Dest [kW]
(a)
(b)
(c)
(d)
(e)
(f)
(g)
(h)

Fig. 8

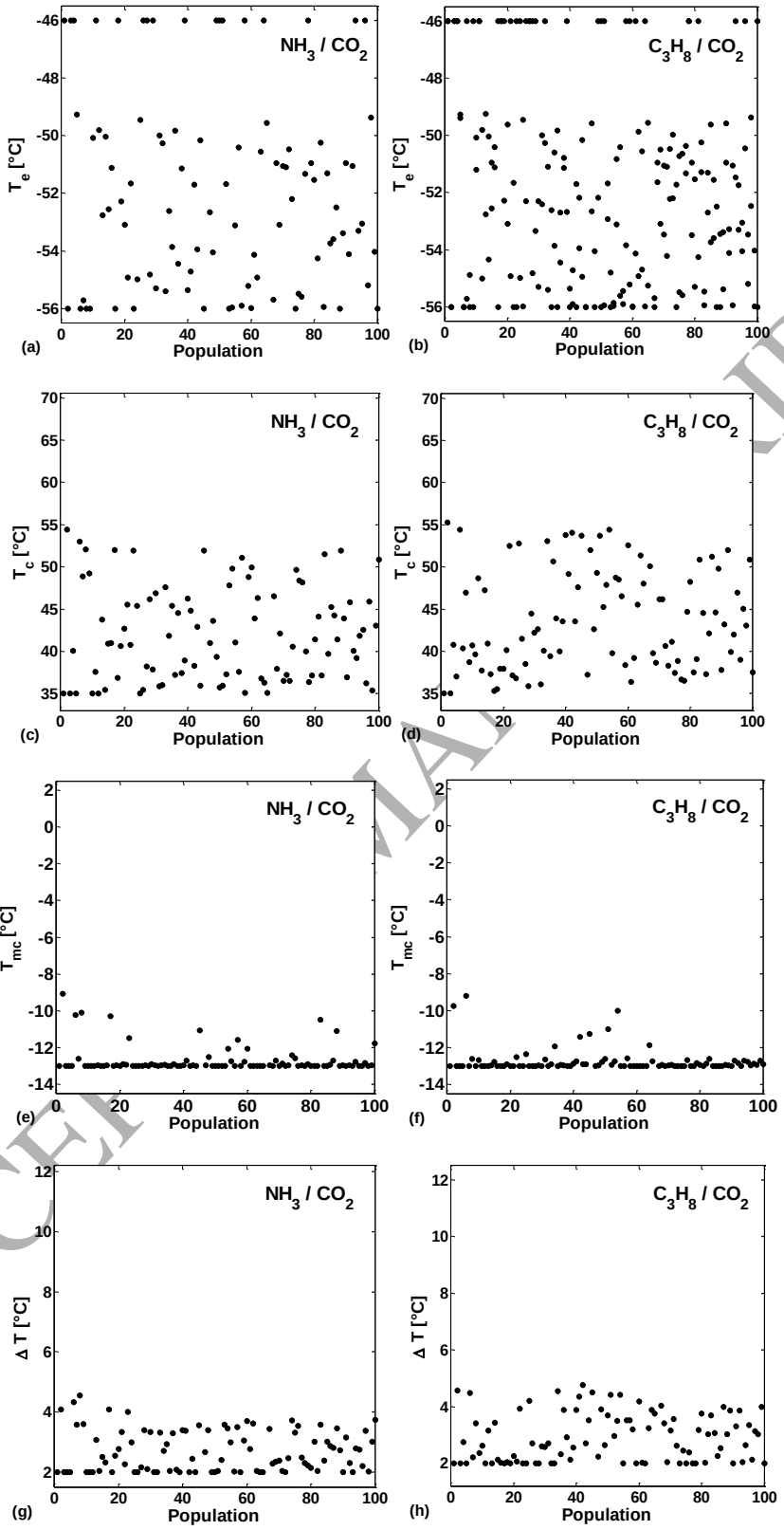

Fig. 9

Table 1:

Specification	Condenser	Evaporator
Lateral pitch (mm)	57	57
Longitudinal pitch (mm)	49.7	49.7
Length of pass (mm)	1000	350
Outer diameter of tube (mm)	12.7	15.9
Tube thickness (mm)	0.889	0.889
Number of tube rows	6	6
Number of fins per 1000 mm	300	200
Fin thickness (mm)	0.25	0.25
Thermal conductivity of tube (W/m K)	52	389

Table 2

Specification	Value
Outer diameter of tube (mm)	25
Tube thickness (mm)	1.65
Number of tubes	16
Number of passes	2
Shell diameter (mm)	200
Baffle spacing (mm)	350
Square pitch (mm)	25.4
Thermal conductivity of tube (W/ m K)	52

Table 3

Parameters	Value
Cooling capacity	40 kW/ 11.5 TR
Ambient temperature	25^{o} C
Cold space temperature	-45^{o} C
Air inlet temperature on condenser	25^{o} C
Air outlet temperature on condenser	30^{o} C
Operating period	15 years
Period of operation per year	6570 h
Annual interest rate	8%
Electricity cost	0.07 $/kWh

Table 4

Selection probability of conduction phase: 0-0.3333
Selection probability of convection phase: 0.3333-0.6666
Selection probability of radiation phase: 0.6666-1
Conduction factor: 2
Convection factor: 10
Radiation factor: 2

Table 5

Objective	Output			
	Total annual cost ($)		Exergy destruction (kW)	
	NH_3/CO_2	C_3H_8/CO_2	NH_3/CO_2	C_3H_8/CO_2
Minimum total annual cost ($)	109592	102645	48.72	52.11
Minimum exergy destruction (kW)	172968	178784	19.79	20.18

Table 6:

	NH_3/CO_2						C_3H_8/CO_2					
	A	B	C	D	E	F	A	B	C	D	E	F
Evaporator temperature (^oC)	-46	-50.04	-51.31	-54.44	-56	-56	-46	-46	-51.2	-52.93	-55.38	-56
Condenser temperature (^oC)	35	35.47	39.73	44.56	49.19	54.42	35	40.37	40.69	45.26	49.77	55.26
LTC condensing temperature (^oC)	2	2.03	2.37	3.3	3.59	4.08	2	2.21	2.63	2.96	3.86	4.57
Cascade temperature difference (^oC)	19.79	23.74	27.84	35.96	42.63	48.72	20.18	23.51	29.22	34.95	43.35	52.11
Total annual cost ($)	172968	149344	129469	114636	110551	109592	178784	155310	125542	112218	104555	102645

Table 7:

	Refrigerant pair (HTC/LTC)	
	NH_3/CO_2	C_3H_8/CO_2
Temperature of evaporator (T_e)	-53.38^o C	-53.48^o C
Temperature of condenser (T_c)	42.90^o C	45.02^o C
Condensing temperature in cascade condenser (T_{mc})	-13^o C	-12.86^o C
Cascade condenser temperature difference (ΔT)	2.76^o C	3.14^o C
Exergy destruction in LTC (kW)	5.53	5.72
Exergy destruction in HTC (kW)	27.95	29.91
Total exergy destruction (kW)	33.48	35.63
Evaporator area (m^2)	296.65	293.04
Cascade condenser area (m^2)	201.51	219.11
Condenser area (m^2)	629.97	523.22
Annual cost ($)	117441.2	111177.71